Studying structural properties of thin film nanostructure of pentoxide vanadium Prepared by reactive DC magnetron sputtering

IOP Conf. Series: Materials Science and Engineering **557** (2019) 012065 doi:10.1088/1757-899X/557/1/012065

Studying structural properties of thin film nanostructure of pentoxide vanadium Prepared by reactive DC magnetron sputtering

M Sh Muhammed[1], M K Kalaf [2], S J Mohammed[3]

[1] Education Mission. Education Department. Salah al-Din. Iraq
[2] Ministry of Sciences and Technology. Baghdad, Republic of Iraq
[3] Tikrit University. Tikrit. Republic of Iraq
E-mail: muhshr@gmail.com

Abstract. In this work, the structural properties of the monocrystalline vanadium pentoxide have been presented. Vanadium pentoxide (V_2O_5) films were deposited by using a DC reactive magnetron sputtering system at working pressure of $8.5x10^{-2}$mbar. The sputtered vanadium atoms were sputtered and oxidized in presence O_2:Ar gas mixture by (5/95,10/90,15/85,20/80,30/70,50/50). Employment of magnetron results in the formation of V_2O_5 in the final samples according to the XRD analysis, increase the roughness and hence surface area of the produced V_2O_5nanostructures. The results of X-rays are shown to us, the deposited films were formed by nanoparticles with average grain size in the range of (52.11nm to 98.03) nm and roughness Ave (nm) in the range of (1.04nm to 8.88nm) . The deposited films are identified to be polycrystalline nature with a cubic structure along ((001), (111)) and ((200)) orientation also MonoV2O5, Cub VO were found as deposited. The texture of the films was observed using SEM and AFM, it was observed that the grain size was increased with increased the O_2 percentage. These improvements in the structural properties of the produced vanadium pentoxide make these nanostructures good candidates for specific applications, such as photo detectors, solar cells, electro chromic smart window and gas sensor.

1. Introduction

Vanadium creates wide range of composites with oxygen which have variation structural and different valence states and founds in a many phases of oxide comprise of vanadium oxide, There are at least 15 variation vanadium oxides communally to now, for example; VO, V_2O_3, VO_2, V_2O_5,V_6O_{13} and so on[1]. V2O5 are known to be the most stable compound form for vanadium metal , but other non-stable stoichiometry can be constrain under particular oxidation conditions.

Different phases of vanadium oxides can be obtained by controlling the deposition method parameters, or by proportion process manipulate, e.g., additional thermal annealing .properties of these phases of vanadium oxides depend on their structure, which determines other properties which exhibit a complex stoichiometric composition[2]. Thin-walled oxide nanoparticles belong to this smart inventory list, and these thin-layer oxide structures have been accelerated for practical applications

such as electronics and optoelectronics. Most of these vanadium oxides are characters for the transfer of semiconductor phases to metal to reversible [3], which is accompanied by large changes in infrared optical properties and their electrical resistance.[4][5]. Vanadium oxide (V/O) structures are a well-known catalyst among various metal oxides, and so many fundamental studies have been developed wide-spreading centering on catalytic oxidation[6]. They show reversible metal-semiconductor transition through a wide band of temperatures depending on the ratio of O/V[7][8], Which results in sudden changes that are accompanied by large changes in infrared optical properties and electrical resistance [7]. The thin layer of vanadium / oxide with defined stoichiometry with the appropriate selection of the network simulation subsystem and the adjustment of many parameters including sedimentation, precipitate rate, pressure and temperature. However, the difficulty of precisely controlling all the parameters and preventing the emergence of defect results in several cases in the stoics is impossible and challenges the synthesis of these oxides as an additional task. Due to these problems, vanadium oxide is mixed with valentine for complex synthesis and research has been reduced. However, vanadium oxide mixed Usually in the process of oxidation / reduction VO2 – V2O5[9]. Vanadium pentoxide (V2O5) has been broadly studied because of its highest oxidation state in the V / O system, a wide band gap, a better stability and its electro thermal effects it is useful for device applications[10]. Except for the pure values of vanadium 0, +2, +3, +4 and +5, respectively, are related to phases V, VO, V2O3, VO2 and V2O5. Two sets of compost properties are identified as stable phases. These series VnO2n-1 and VnO2n + 1 are defined as magnetism. [11][12] , Wesley phases, respectively, and they connect the three most common phases, V_2O_3, VO_2 and V_2O_5[11][13][14]. The working mechanism of electro chromic materials consists of electrolyte, intercalated mobile ions which performs intercalation/de intercalation while a potential difference is applied. For this purpose, layered structure of V2O5 is a promising material. The most commonly used phases, which found in wide range of applications due to their novel properties, are the VO, VO2, V2O3, and V2O5 oxide phases[15].

2. Experimental details

Vanadium pure was chosen as the primary material to study for this project. Sputtering processes normally uses argon gas because it does not react with the target material allowing thin films to be formed. The addition of a gas that reacts with the target material, such as oxygen, will form compounds of the material and the reactant. To determine how vanadium oxide is formed using reactive magnetron sputtering a reactive gas test was performed. Because the sputtering system uses a DC power supply that allows both voltage and current to float while maintaining constant power, the target voltage can be easily measured and used to infer changes in the impedance of the sputtering plasma. The gun in which the target is mounted is designed to provide a narrow range of impedance to the power supply. With the addition of a reactive gas the impedance of the target changes. Using the fixed conditions of 660V of DC power and a chamber pressure of 0.08 mb while introducing increased amounts of oxygen the voltages were recorded. Figure 1 illustrated the outcome of this experiment

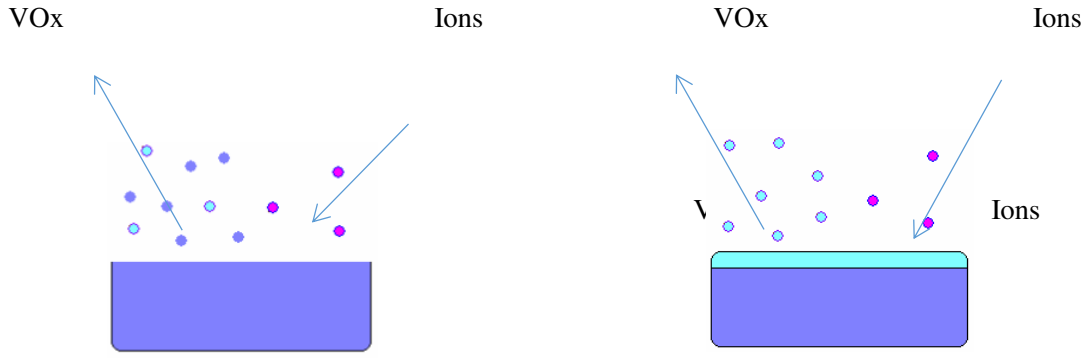

Figure 1. (a) Fully Oxidized Phase. (b) Metallic Phase

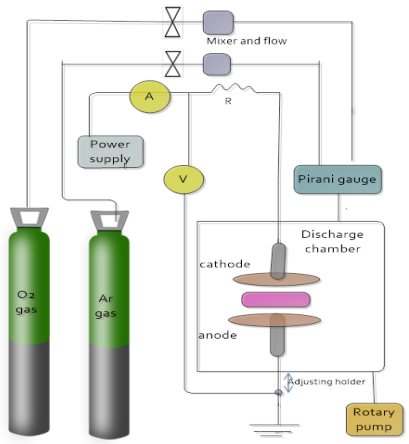

Figure 2. The main experimental set-up used in this work.

3. Results

Figure 3 additionally shows that there are at145, 198, 287, 308, 413, 491, 535 and 1002 cm-1 bands of crystalline V2O5 nanoparticles. [16] The formation of nanoparticles for catalysts with a V V7.7 nm-2 load or more, which is related to the surface coating of a layer (~ 8 V nm-2). [17] The supported V2O5 bands at 491 and 535 cm 1 are wide, while the 705 cm-1 sample does not exist for the V2O5 crystal, suggesting that this V2O5 NP support is not large and well-ordered. All supported AMV catalysts have a Raman group of 1035 cm-1, which extends to Vagabond (VVO) from the surface of the oligomer, an exo VO4 [18,19,20-21] Sharp tapes at 140, 194, 283, 302, 404, 482, 528, 705, and 998 cm-1 are formed from crystalline V2O5 nanoparticles. The peaks at284 and 401 cm-1 indicate that they have vibrational vibrational results V = O. Vibrational vibrations of V-O-V bonds and 3D overlapping V3-O bonds are obtained in 487 [22]. These bands are asymmetric and symmetric, respectively, to the vibrational vibrational states V-O, V-O-V and V = O. The FT-IR spectrum was packed with 100 watts of RF power at 477.21 cm, 1 506.17 cm-1 and 617.16 cm-1. These are vibration banding vibrations of deformation of the O-V gradient and the band of 1046.65 cm-1 relative to the V = O bond [23].

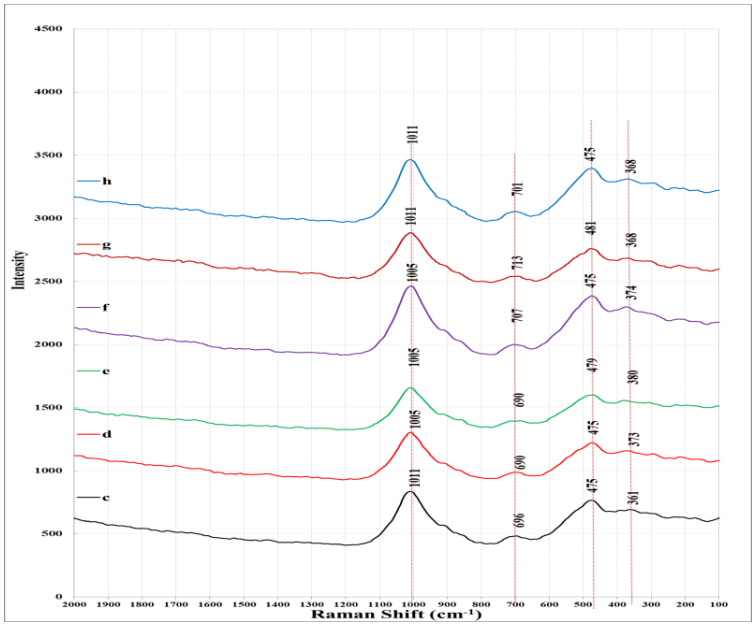

Figure 3. shows the Raman spectrum of vanadium oxide films produced by the O2: Ar ratio.

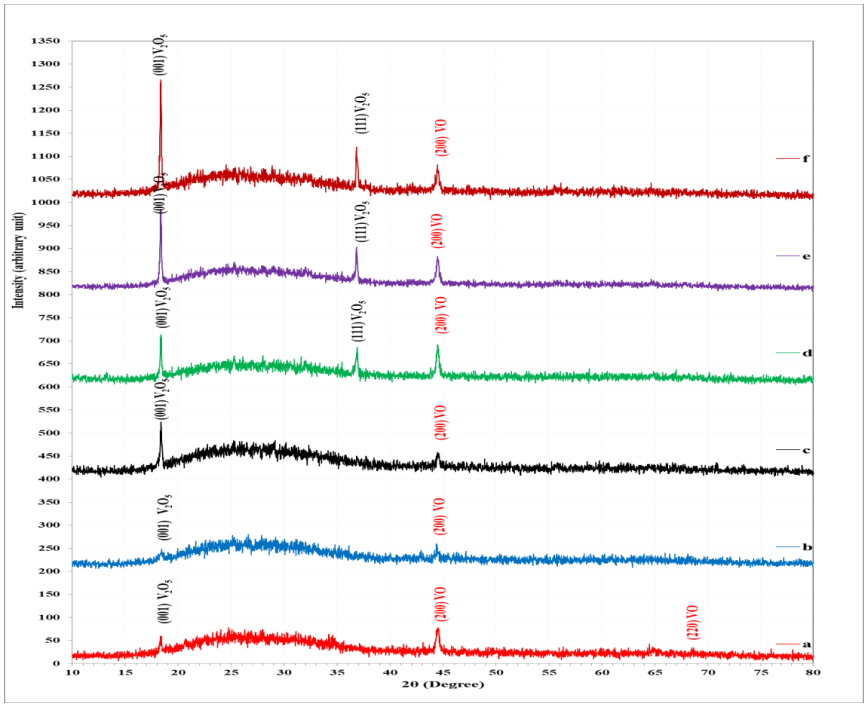

Figure 4. X-ray diffraction patterns for a thin sheet of vanadium deposited with different ratios of O_2: Ar.

Table 1. X-ray diffraction patterns for a thin sheet of vanadium covered with different ratios of O_2: Ar

	2θ (Deg.)	FWHM (Deg.)	d_{hkl} Exp.(Å)	G.S (nm)	d_{hkl} Std.(Å)	hkl	Phase	card No.
a	18.3105	0.2826	4.8413	28.5	4.3830	(001)	Mono. V_2O_5	96-901-2222
	44.5100	0.4037	2.0339	21.3	2.0310	(200)	Cub. VO	96-900-8767
b	18.4316	0.3633	4.8098	22.2	4.3830	(001)	Mono. V_2O_5	96-901-2222
	44.3889	0.5248	2.0392	16.3	2.0310	(200)	Cub. VO	96-900-8767
c	18.3509	0.2422	4.8307	33.2	4.3830	(001)	Mono. V_2O_5	96-901-2222
	44.4697	0.2825	2.0357	30.4	2.0310	(200)	Cub. VO	96-900-8767
d	18.3105	0.1615	4.8413	49.8	4.3830	(001)	Mono. V_2O_5	96-901-2222
	36.8051	0.2825	2.4400	29.6	2.4434	(111)	Mono. V_2O_5	96-901-2222
	44.4697	0.3633	2.0357	23.6	2.0310	(200)	Cub. VO	96-900-8767
e	18.3509	0.2018	4.8307	39.9	4.3830	(001)	Mono. V_2O_5	96-901-2222
	36.6840	0.2422	2.4478	34.6	2.4434	(111)	Mono. V_2O_5	96-901-2222
	44.4697	0.3229	2.0357	26.6	2.0310	(200)	Cub. VO	96-900-8767
f	18.3509	0.2018	4.8307	39.9	4.3830	(001)	Mono. V_2O_5	96-901-2222
	36.6840	0.2018	2.4478	41.5	2.4434	(111)	Mono. V_2O_5	96-901-2222
	44.4697	0.3633	2.0357	23.6	2.0310	(200)	Cub. VO	96-900-8767

The X-ray diffractions of the Vanadium target is also displayed . The target material exhibits peaks corresponding to the mono V2O5 phase at 2θ = 18.3105°, 18.4316°,18.3509°, 36.8051°, 36.64840°, and 36.6840°, direction identify with standard peaks[card. No(96-901-2222)]. It are belongs to Pmmn space group having lattice parameters as a = 11.544 A°, b = 3.571 A° and c = 4.383 A°. The XRD pattern illustrates that the (V2O5) films have polycrystalline (111), (001) and The X-ray diffractions of the Vanadium target is also displayed cub(VO) . The target material exhibits peaks corresponding to the cub VO phase at 2θ=44.5100°,44.3889°,44.4697°, direction identify with standard peaks[card96-900-8767]. It are belongs to Pmmn space group having lattice parameters as a=4.0620A°. The XRD pattern illustrates that the (V2O5) films have polycrystalline (200). also, note that increases the different O_2:Ar ratio ., leads to peak intensity increases (i.e. increase films crystallinity). This might be due to a change in its phase or crystal structure as deposition rate varied. Also, increasing RF power making increases in grain size, as shown in Table 1, this may be due to the enhancement of films crystallinity. So, improved the crystalline of the films by increasing grain size to decrease the number of grain boundaries. A significant amount of line broadening which is a characteristic of nanoparticles. All the XRD patterns show same behavior where the FWHM decreases with increase of the different O_2:Ar ratio .with increasing the crystallite size. [180,181].

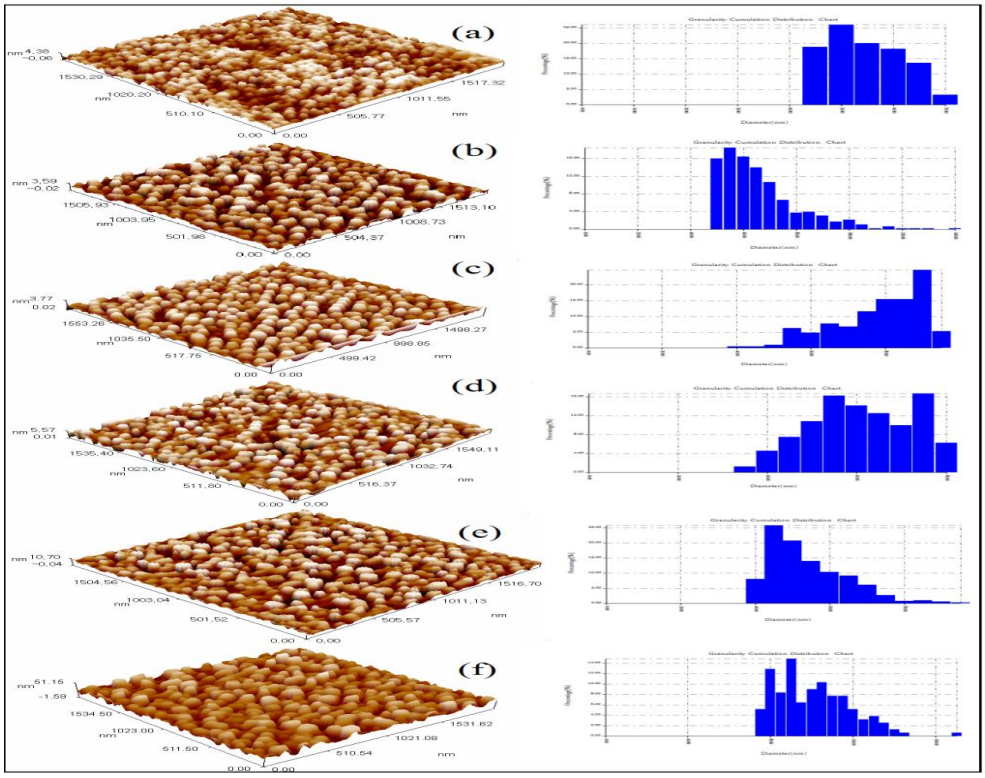

Figure 5. 3D AFM image and their granularity accumulation distribution for vanadium thin films at different O_2:Ar ratio.

The values of grain sizes for Vanadium oxide thin films are given in Table 2. This table increases grain size between (52.11-98.03) nm and the RMS roughness between (1.04 and 8.88) nm with increases O_2/Ar ratio. The images at the low pressure confirm that the films are uniform and the substrate surface is well covered with grains that are nearly uniformly distributed. When increasing the gas pressure. The possibility of some small grains agglomerated to form greater grains as a consequence. The deposited film exhibited small nicely combined with coalescence of some columnar grains at few places. The decrease in surface roughness of the deposited films with higher pressures is due to the growth of grains with favorable orientation dictated by surface and grain boundary diffusivity, ad-atom mobility, film thickness and induced thermal stress. This behavior is similar and agrees with the results obtained in the reference.

Table 2. of AFM 3D image and its gravitational accumulation distribution for vanadium thin sheets with different O2: Ar ratios

O_2:Ar ratio	Average Diameter (nm)	RMS roughness (nm)	Roughness Ave.(nm)
5/95	52.11	0.881	1.04
10/90	63.57	0.902	1.04
15/85	75.97	0.845	0.991
20/80	58.52	1.31	1.53
30/70	51.47	2.42	2.85
50/50	98.03	7.37	8.88

4. Conclusions:

In this paper, an analysis of the structural properties of vanadium powder oxide produced by reactive spectrometry has been observed. An increase in the surface roughness of the samples was observed with an increase in the ratio of the mixture of gases. This allows for the use of samples prepared in the use of gas sensors.

References

[1] Schneider K 2015 *Structural and optical properties of VOx thin films. Archives of Metallurgy and Materials* **60.2** 957-961

[2] Golan G et al 2004 *Investigation of phase transition mechanism in vanadium oxide thin films. Journal of Optoelectronics and Advanced Materials* **6.1** 189-195

[3] M E A Warwick and R. Binions *Advances in thermochromic vanadium dioxide films J. Mater. Chem.* **2. 10** 3275–3292

[4] Donev Eugenii U 2008 *Metal-semiconductor transitions in nanoscale vanadium dioxide-thin films, subwavelength holes, and nanoparticles* PhD Thesis

[5] Liu Yueyan et al.*2016 Effect of annealing temperature on the structure and properties of vanadium oxide films. Optical Materials Express* **6.5** 1552-1560

[6] Zou Mengyang *2015 Deposition Methods and Thermoresistive Properties of Vanadium Oxide and Amorphous Silicon Thin Films* PhD Thesis. University of Dayton.

[7] M Farahmandjou *2017 Chemical Synthesis of Vanadium Oxide (V2O5) Nanoparticles Prepared by Sodium Metavanadate," J. Nanomedicine Res* **5.1** 2–5

[8] Lamsal Chiranjivi Ravindran M 2013 *Optical properties of vanadium oxides-an analysis. Journal of materials science* **48.18** 6341-6351

[9] Urena Begara, Ferran Crunteanu, Aurelian Raskin, Jean-Pierre 2017 *Raman and XPS characterization of vanadium oxide thin films with temperature. Applied Surface Science* **403** 717-727

[10] Vijayakumar Yelsani et al 2015 *Influence of the substrate temperature on the structural, optical and thermoelectric properties of sprayed V2O5 thin films. Material in technologies* **49.2** 17

[11] Ramplberg Geert et al 2015 *In situ X-ray diffraction study of the controlled oxidation and reduction in the V–O system for the synthesis of VO 2 and V 2 O 3 thin films. Journal of Materials Chemistry* C3 **43** 11357-11365

[12] Jeong Jaewoo et al 2013 *Suppression of metal-insulator transition in VO2 by electric field–induced oxygen vacancy formation Science* **339.6126** 1402-1405

[13] Masina Bathusile N et al2015 Optimizing the synthesis of vanadium–oxygen nanostructures by plasma plume dynamics using optical imaging. *Optical Engineering* **54.3** 037106

[14] Fay Alexander 2005 *Engineering in vernetzten, offenen, durchgängigen Systemen (Engineering in Linked and Open Systems). at-Automatisierungstechnik* **53.4-5** 205-210
[15] Yimam Elias 2015 *Fabrication of Vanadium Oxide Nanoparticles by Pulsed Laser Ablation*
[16] Carrero Carlos A et al 2013 *Anomalous reactivity of supported V 2 O 5 nanoparticles for propane oxidative dehydrogenation: influence of the vanadium oxide precursor. Dalton Transactions* 42.35 12644-12653
[17] Deo Goutam Wachs Israel E 1994 *Reactivity of supported vanadium oxide catalysts: partial oxidation of methanol. Journal of catalysis* **146.2** 323-334
[18] Tian Hanjing Ross Elizabeth I 2 Wachs Israel *E2006 Quantitative determination of the speciation of surface vanadium oxides and their catalytic activity*. *The Journal of Physical Chemistry B* **110.19** 9593-9600
[19] Argyle Morris D et al 2002 *Effect of catalyst structure on oxidative dehydrogenation of ethane and propane on alumina-supported vanadia*. *Journal of Catalysis* **208.1** 139-149
[20] Went Gregory T Oyama S Ted Bell Alexis T *1990 Laser Raman spectroscopy of supported vanadium oxide catalysts. Journal of physical chemistry* **94.10** 4240-4246
[21] Olthof Bryan et al 2000 *Effects of support composition and pretreatment conditions on the structure of vanadia dispersed on SiO2, Al2O3, TiO2, ZrO2, and HfO2. The Journal of Physical Chemistry B* **104.7** 1516-1528
[22] Lee Se-Hee et al 2003 *Raman spectroscopic studies of amorphous vanadium oxide thin films. Solid State Ionics* **165.1-4** 111-116
[23] Murgia Viviana et al 2006 *Sol–gel synthesis of V2O5–SiO2 catalyst in the oxidative dehydrogenation of n-butane. Applied Catalysis A: General* **312** 134-143